Chapter 6

TOPEX/Poseidon Sea Level Height Anomaly

Besides the Complex EOF analysis in time domain [Horel, 1984] of the synthetic data discussed in Chapter 3.5 and in Chapter 5, we have successfully performed Complex EOF and EOF analysis on different geophysical data sets, viz., the Reynolds SST data ([Reynolds, 1993] and [Reynolds and Smith, 1994]) in both available variants (weekly and monthly); and TOPEX/Poseidon derived sea level height anomaly data again in both variants (weekly and monthly).

However in this chapter we will present results of Complex EOF and EOF analysis only of the TOPEX/Poseidon derived monthly sea level height anomaly using the ($1^o \times 1^o$) global monthly data for the period 1993-2003 (11 years) downloaded from the website of the Center for Space Research, University of Texas, Austin.

All the analyses presented in this chapter as well as in Chapter 5, except for *Example 4#* in the latter chapter - have beenn carried out using the software presented in Appendix A without any changes on a 128 Mb RAM linux personal computer, Kapila. Because of the large number of temporal elements ($= 4096$), *Example 4#* was run on the 4 Gb RAM Sun work station, Sarayu, after suitably changing the dimensions of some variables in the computer program *ceof-vec.f*. It may be mentioned that even *Example 4#* was initially successfully run on a 32 Mb RAM, 2 Gb hard disk personal computer, Aneerudh. That was before we changed our strategy **from** using the spatial covariance matrix **to** using the temporal covariance matrix - for determininng the eigen values and eigen vectors. The change in strategy was for the pupose of runtime optimization since in the actual geophysical data, generally the number of spatial elements is much, much larger than the temporal elements; unlike the synthetic data of Horel [1984].

The Complex EOF analysis of the raw downloaded TOPEX/Poseidon monthly sea level height anomaly data was used to produce the Hov-moller diagrams, Figure 6.9 and Figure 6.10, of sea

level height anomaly in the Indian Ocean at annual periodicity, constructed from the first pair of spatial and temporal complex empirical orthogonal functions, viz, CEOF 1.

The EOF analysis of sea level height anomaly in the Indian and Pacific Oceans at interannaual time scales, was performed after removing the annual cycle from the downloaded time series data at each grid point. To remove the annual cycle, long term (over the 11 years) monthly means at each grid point were calculated and subtracted from the individual months of the 132 month (11 years) time series at the grid point following Davis [1976]. In a similar analysis Chambers et al. [1999] had removed both the annual as well as the semi-annual cycles by fitting sinusoids with annual and semi-annual periodicities using the least squares method.

The Complex EOF analysis of sea level height anomaly in the Indian and Pacific Oceans at interannual time scales was performed after removing the annual cycle from the raw downloaded data, just like in the case of EOF analysis discussed above, and then low pass filtering the data using the filter of White [2000a]. Also following Horel [1984] one tenth of each time series (12 months data) at the beginning and end of the record were deleted to avoid end effects.

Both the EOF as well as Complex EOF analysis of sea level height anomaly in the Indian Ocean at interannual time scales showed the signature of the El Ninos of 1994-95 and 1997-98, the latter being the El Nino of the century, and the Indian Ocean dipole ([Saji et al., 1999] and [Webster et al., 1999]). The La Nina of the century 1998-99 has been captured by the second pair of spatial and temporal EOFs in the Pacific Ocean.

We note that our results depicted in the form of figures in this chapter are consistent with authoritative published reports.

To our knowledge, EOF analysis applied to the Indian Ocean is discussed in Picaut et al. [2002], Kantha and Clayson [2000], Potemra and Lukas [1999] and also in Rao et al. [2002].

To our knowledge, Complex EOF analysis applied to the Indian Ocean, is discussed in White [2000a], Basu et al. [2000], Eigenheer and Quadfasel [2000], Perigaud and Delecluse [1993], Perigaud and Delecluse [1992] and also in Rao et al. [2002].

Kishtawal et al. [2001] is perhaps the only paper using Complex EOF analysis communicated from India. It is used in the meteorological context; in the oceanographic context there is none.

While Wallace [1972] is the pioneer in the use of Complex EOF analysis in the meteorological context, Barnett [1983] and Barnett [1984] is the pioneer of such use in the oceanographic context.

6.1 Complex EOF Analysis: TOPEX/Poseidon - Indian & Pacific Oceans

.

.

Table 6.1 Complex EOF analysis - TOPEX/Poseidon data - Indian Ocean: Percentage of variance explained by different empirical modes at *interannnual* time scales. $\nu = 15.6$, indicating that the varimax rotated modes need not be considered

Mode	Percentage Variance Explained	Cumulative Variance Explained
1	75.2	75.2
2	14.0	89.2
3	7.2	96.4
4	1.9	98.3
5	1.2	99.5

Table 6.2 Complex EOF analysis - TOPEX/Poseidon data - Pacific Ocean: Percentage of variance explained by different empirical modes at *interannnual* time scales. $\nu = 23.3$, indicating that the varimax rotated modes need not be considered

Mode	Percentage Variance Explained	Cumulative Variance Explained
1	78.1	78.1
2	15.2	93.3
3	3.9	97.2
4	1.8	99.0
5	0.7	99.7

Figure 6.1 Low Pass Filter Response functions of: *(a)* The filter used by White [2000a] to study the interannual variablity of sea surface temperature (SST) and TOPEX/Poseidon derived sea level height anomaly data, and *(b)* The linear taper of Walters and Heston [1982] used for removing tidal period variations from time series data - both the filters are available in our computer program *hilbert.f*. In the latter case the characteristics of the linear taper filter can be set through the specification file *hilbert.spc*

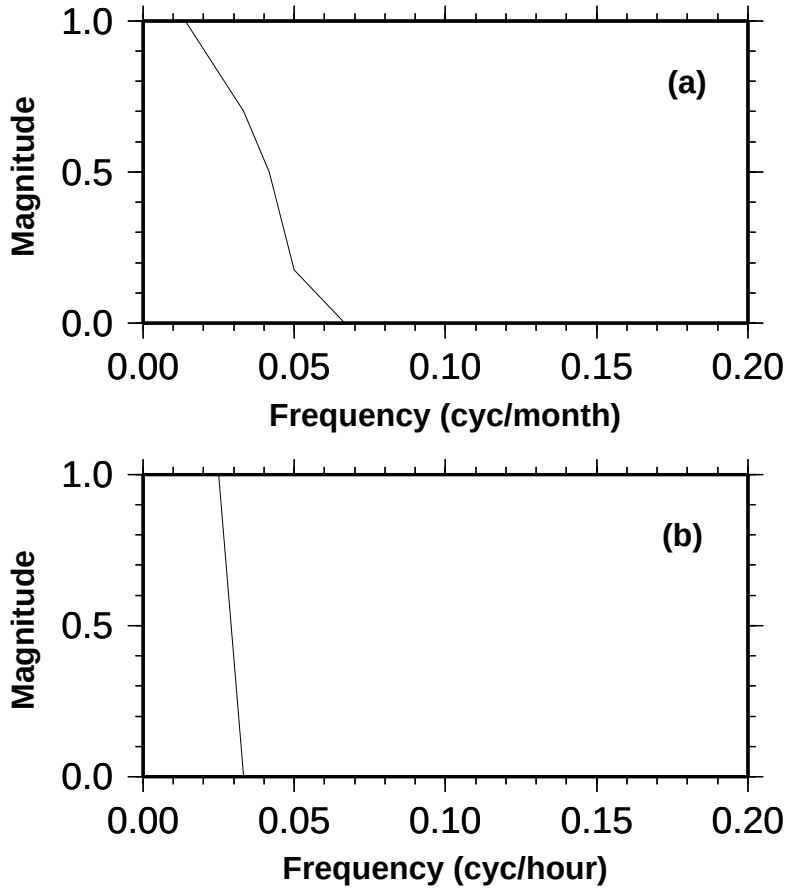

Figure 6.2 Complex EOF analysis: TOPEX/Poseidon sea level height anomaly data - Spatial amplitude of CEOF-1 at *interannual* time scales. Note the large amplitudes in the sea level at the two poles of the Indian Ocean dipole, one to the south of Sumatra and western Java & the other pole at 9^oS, 58^oE. That this is the signature of the dipole is seen from Figure 6.3, which shows the phase difference between the poles to be $\approx 205^o$ close to the theoretical value of 180^o. The orientation of the ridge associated with the latter pole, is consistent with Rossby wave propagation, which theoretically have decreasing phase speeds with increasing latitude; Indian Ocean

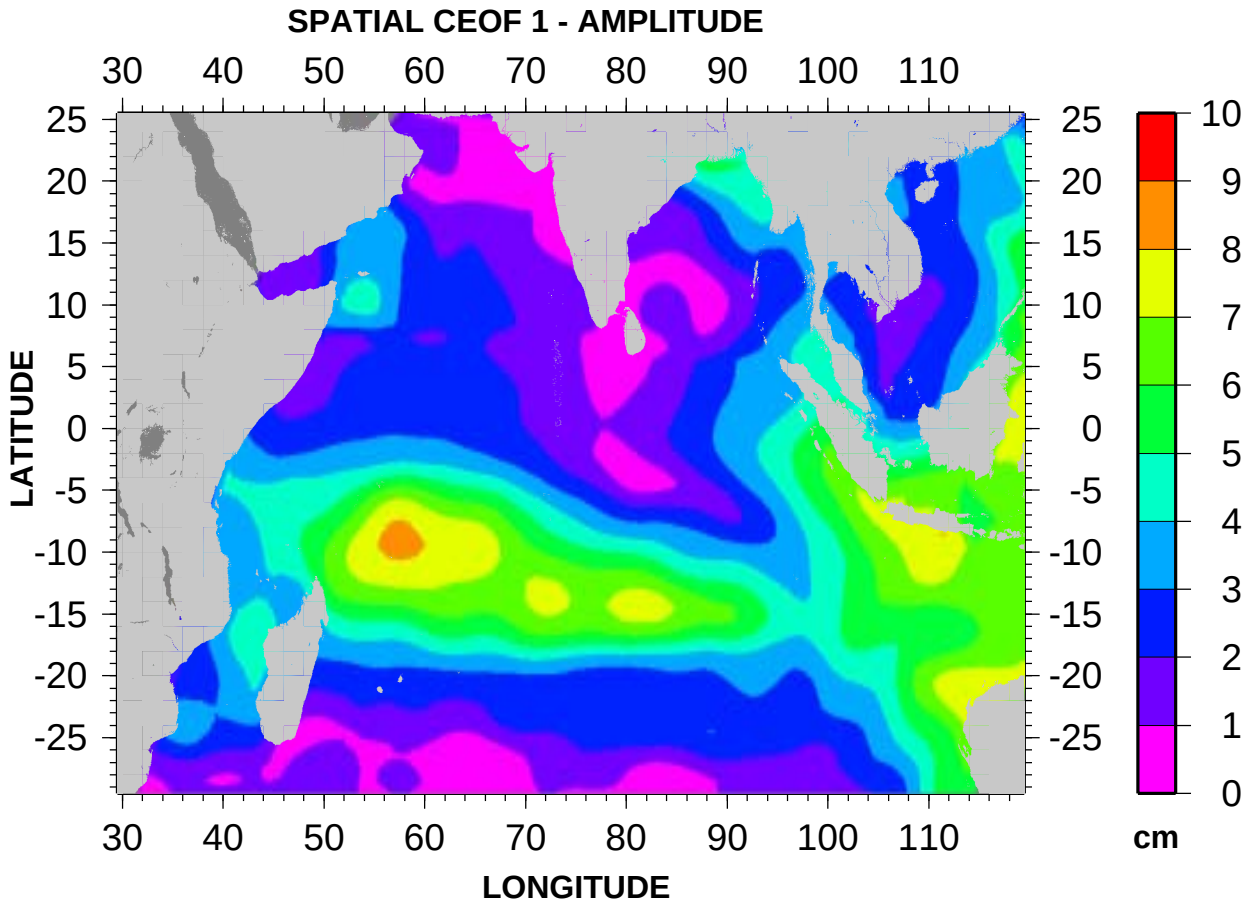

Figure 6.3 Complex EOF analysis: TOPEX/Poseidon sea level height anomaly data - Spatial phase of CEOF-1 at *interannual* time scales; Indian Ocean

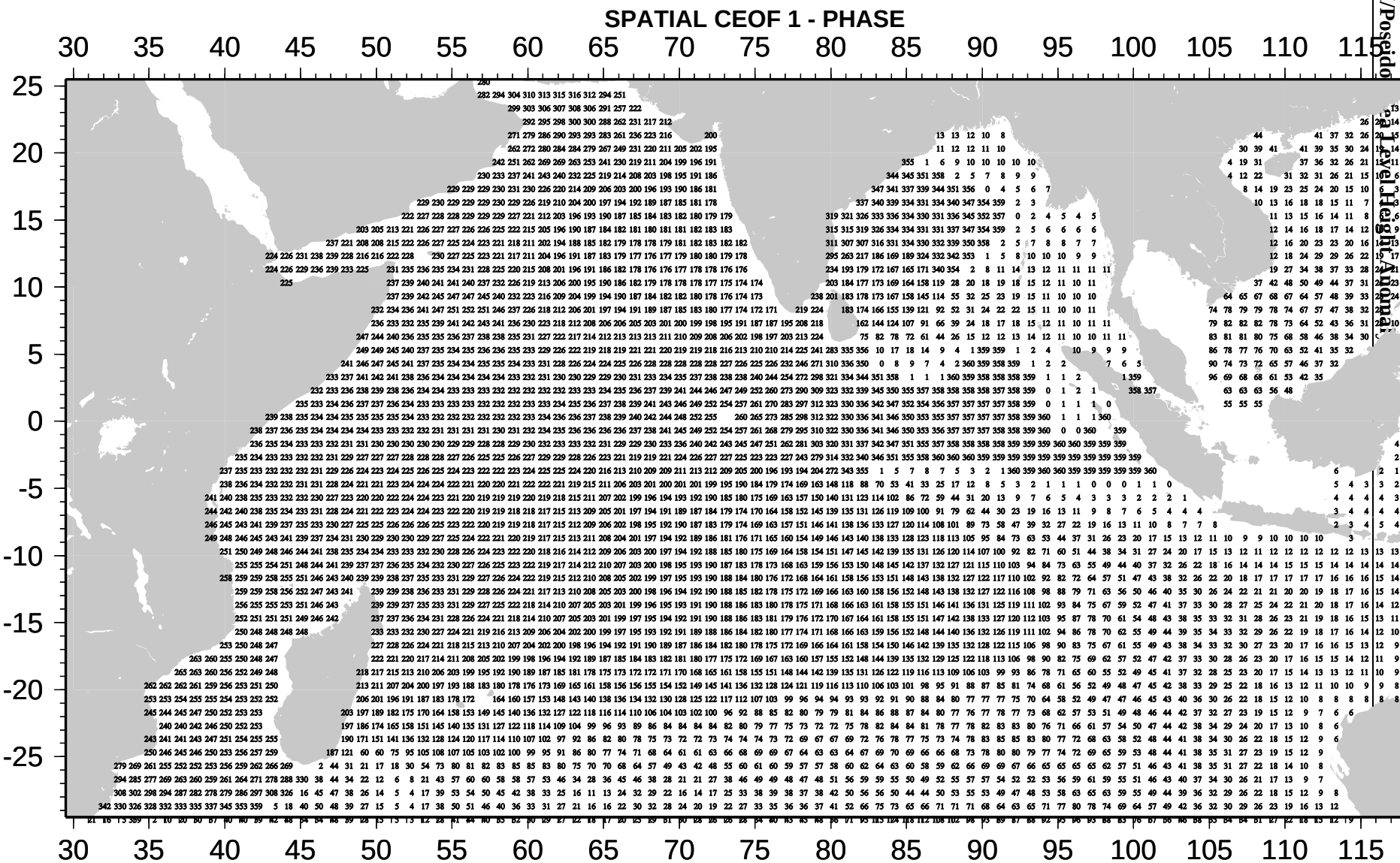

Figure 6.4 Complex EOF analysis: TOPEX/Poseidon sea level height anomaly data - Temporal amplitude & phase of CEOF 1&2 at *interannual* time scales; Indian Ocean

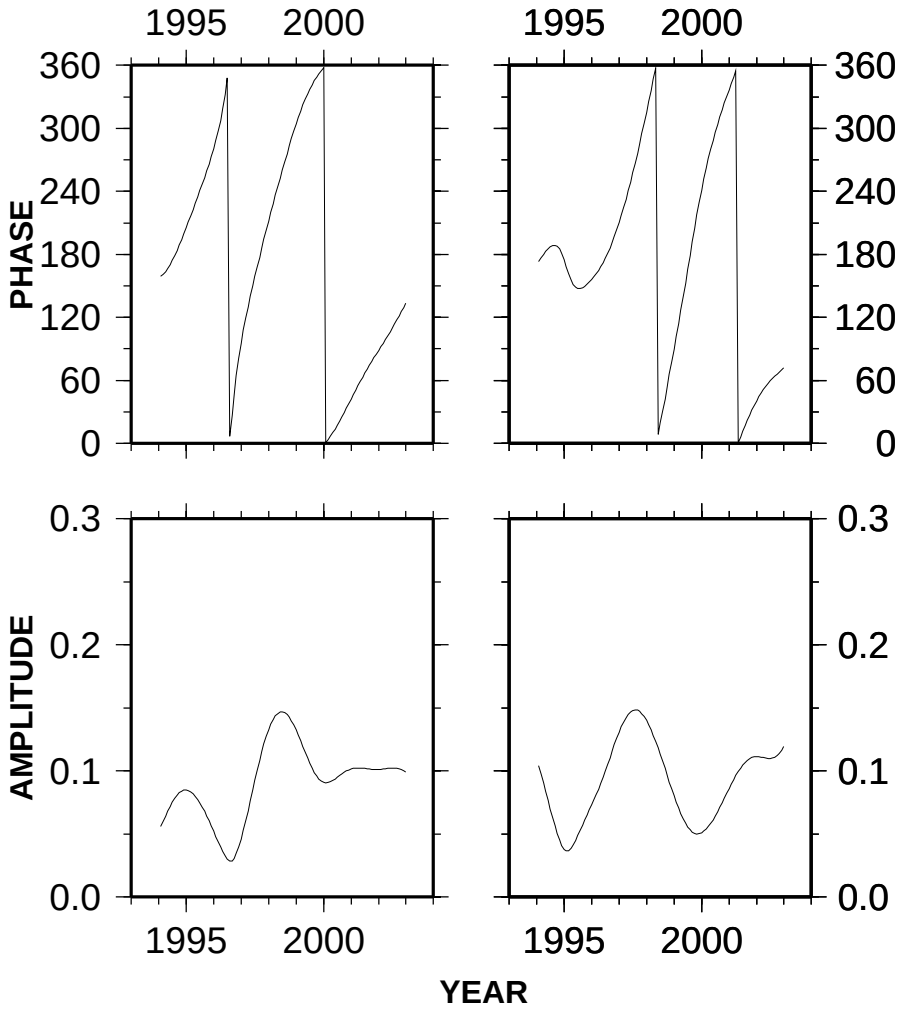

Figure 6.5 Complex EOF analysis: TOPEX/Poseidon sea level height anomaly data - Spatial amplitude of CEOF-1 at *interannual* time scales; Pacific Ocean

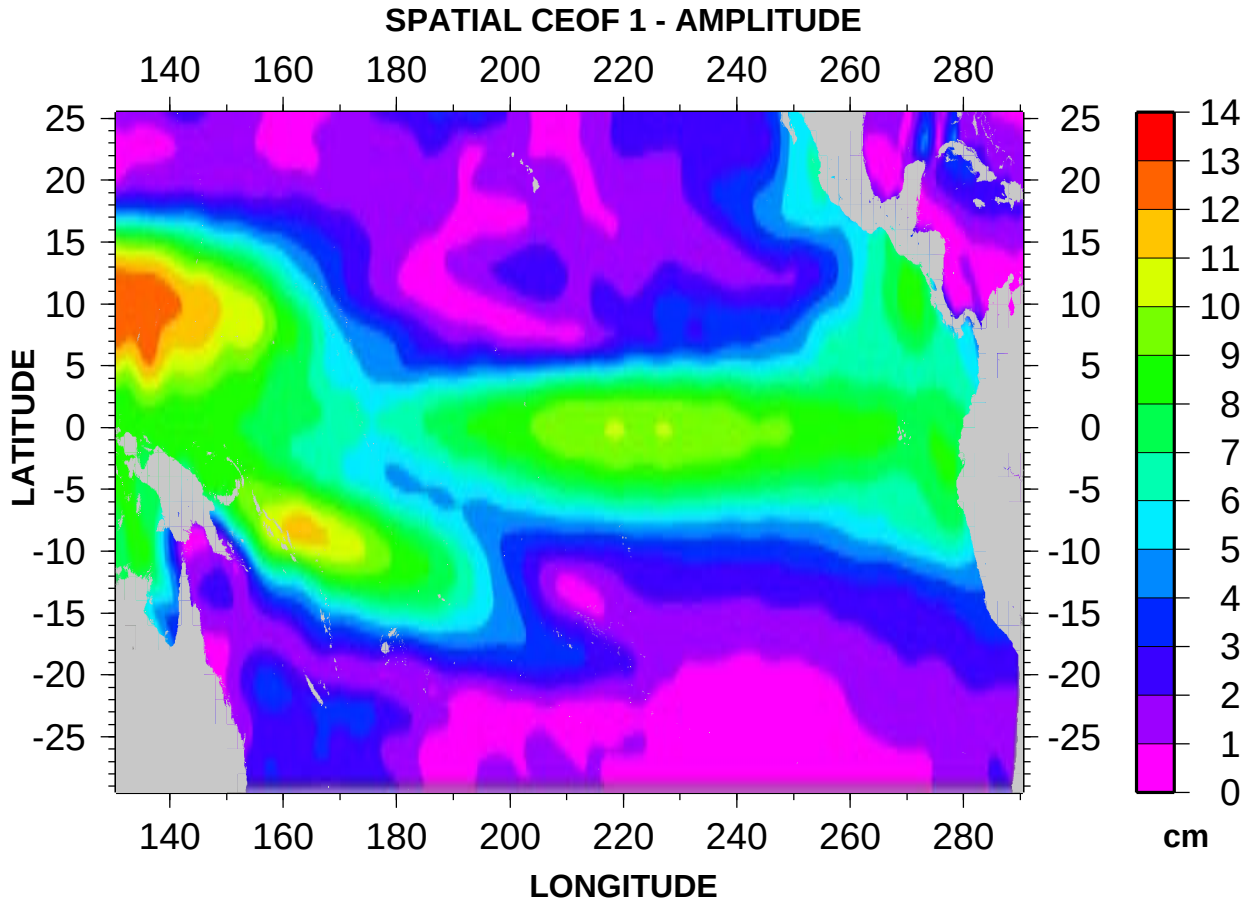

Figure 6.6 Complex EOF analysis: TOPEX/Poseidon sea level height anomaly data - Temporal amplitude & phase of CEOF 1&2 at *interannual* time scales; Pacific Ocean

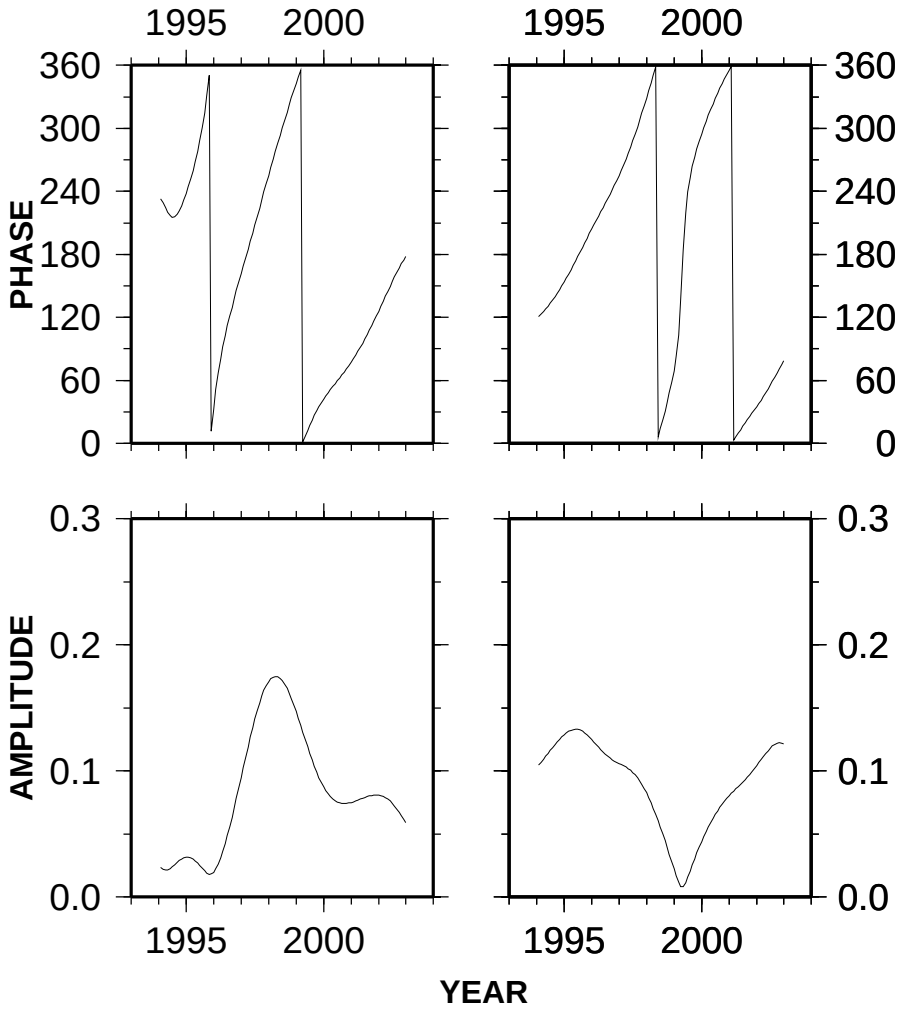

6.2 EOF Analysis: TOPEX/Poseidon - Indian & Pacific Oceans

Table 6.3 EOF analysis - TOPEX/Poseidon data - Indian Ocean: Percentage of variance explained by different empirical modes at *interannnual* time scales. $\nu = 33.5$, indicating that the varimax rotated modes need not be considered. Ten modes were considered

Mode	Percentage Variance Explained	Cumulative Variance Explained
1	35.4	35.4
2	9.6	45.0
3	7.5	52.5
4	6.1	58.7
5	3.9	62.5

.

Table 6.4 Complex EOF analysis - TOPEX/Poseidon data - Pacific Ocean: Percentage of variance explained by different empirical modes at *interannnual* time scales. $\nu = 30.6$, indicating that the varimax rotated modes need not be considered. Ten modes were considered

Mode	Percentage Variance Explained	Cumulative Variance Explained
1	43.8	43.8
2	14.9	58.7
3	7.3	66.0
4	5.1	71.0
5	2.8	73.9

.

Figure 6.7 Complex EOF analysis: TOPEX/Poseidon sea level height anomaly data - Hov-moller diagrams of CEOF-1 at interannual time scales at different latitudes (westward propagating Rossby waves $\approx 7cm/s$ consistent with White [2000a]); Indian Ocean

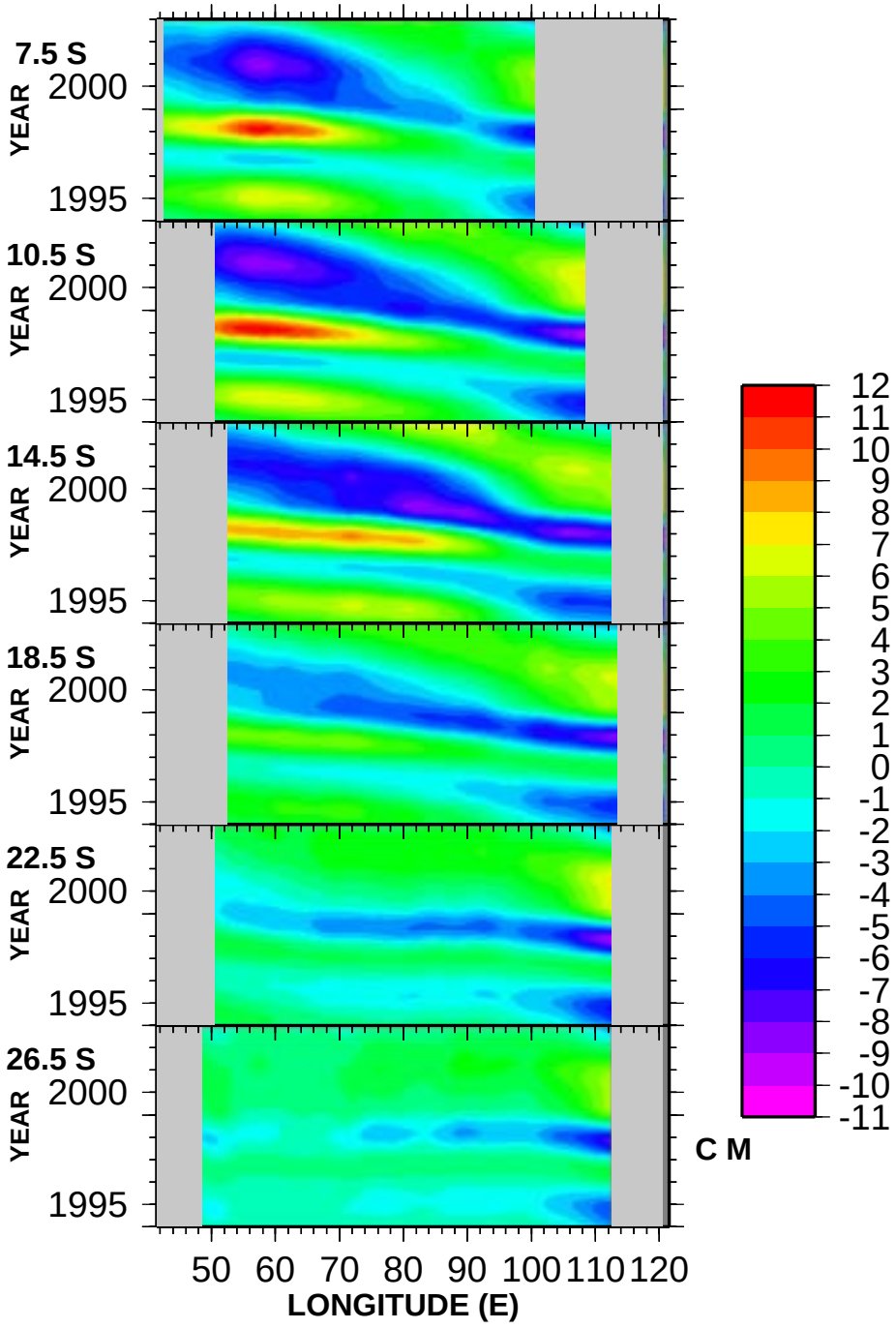

Figure 6.8 Complex EOF analysis: TOPEX/Poseidon sea level height anomaly data - Hov-moller diagrams of CEOF-1 at *interannual* time scales at the Equator (eastward propagating Kelvin wave); and at 7.5^{o}S (westward propagating Rossby wave) both $\approx 7cm/s$; Indian Ocean

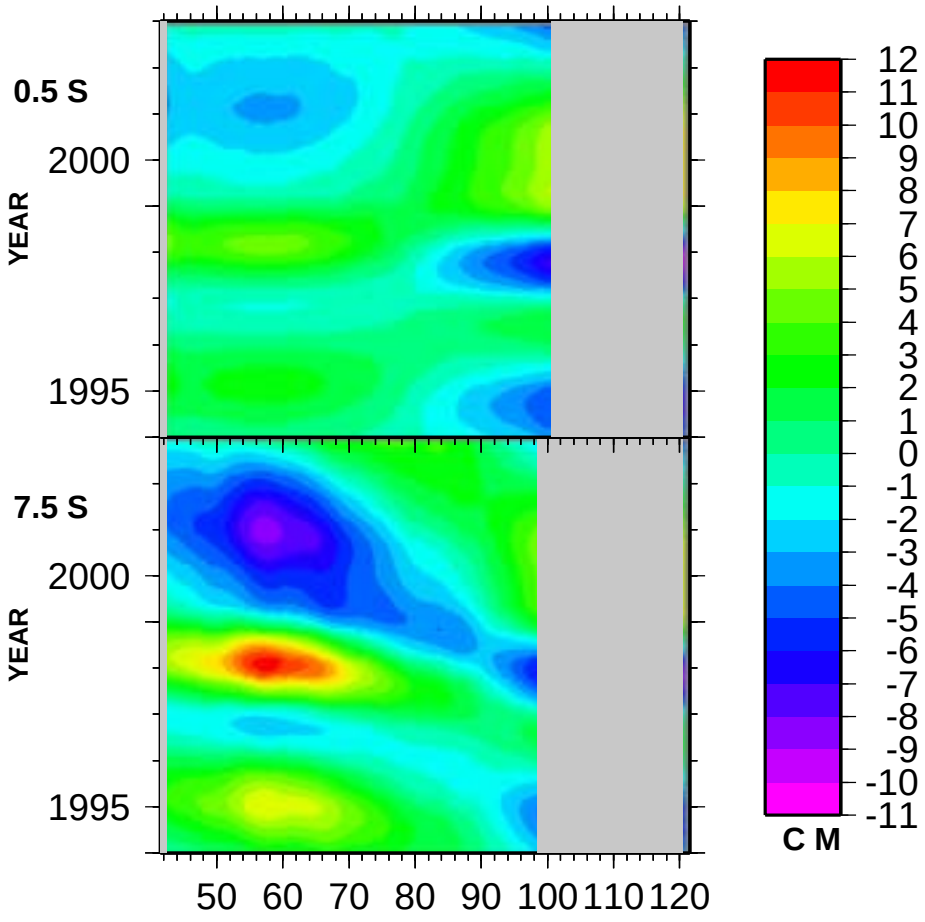

Figure 6.9 Complex EOF analysis: TOPEX/Poseidon sea level height anomaly data - Hov-moller diagrams of CEOF-1 at *annual* time scales at different latitudes (westward propagating Rossby waves $\approx 27 cm/s$) consistent with Basu et al. [2000]; Indian Ocean

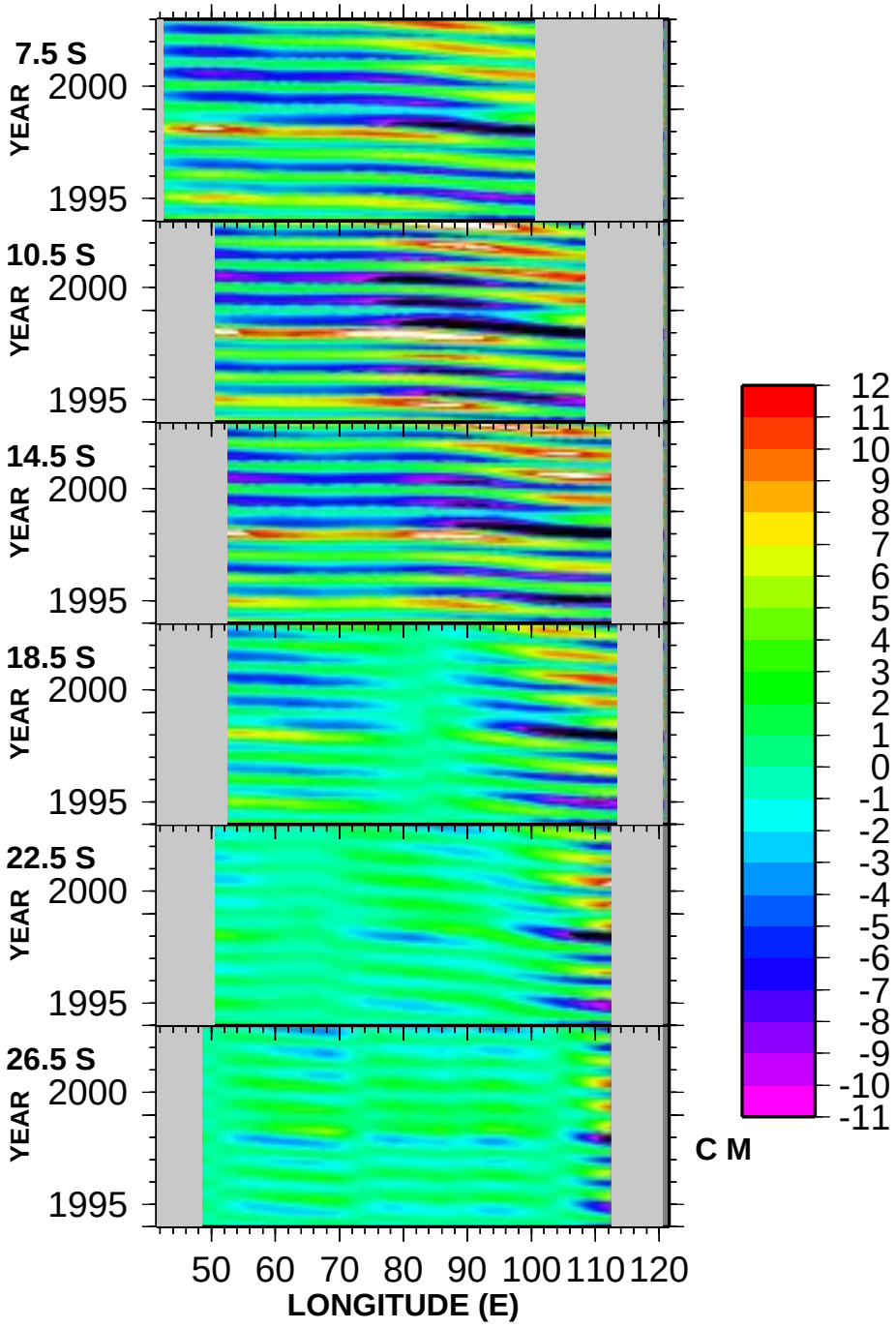

Figure 6.10 Complex EOF analysis: TOPEX/Poseidon sea level height anomaly data - Hov-moller diagrams of CEOF-1 at *annual* time scales at the Equator (eastward propagating Kelvin wave $\approx 54 cm/s$) and; at 7.5°S (westward propagating Rossby wave $\approx 27 cm/s$) consistent with Basu et al. [2000]; Indian Ocean

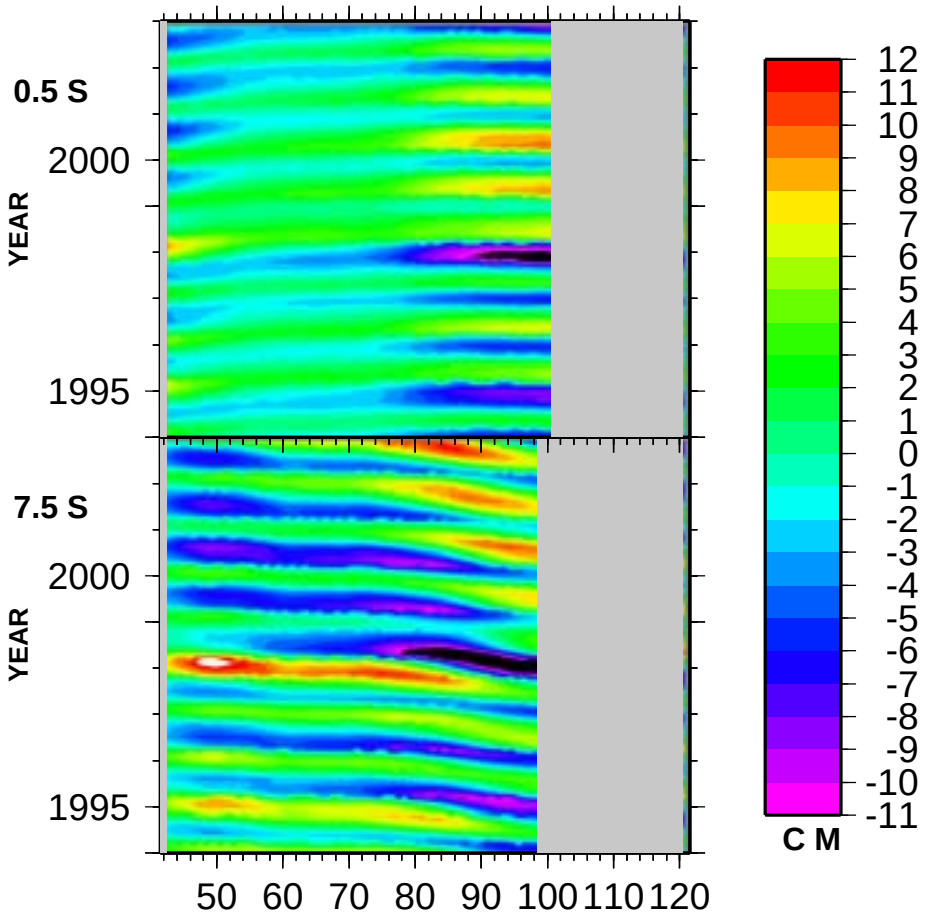

Figure 6.11 EOF analysis: TOPEX/Poseidon sea level height anomaly data - spatial EOF-1 elevation at *interannual* time scales consistent with Chambers et al. [1999]. The two poles of the Indian Ocean dipole are easily recognized from the large negative values of sea level off southern Sumatra (cooling) and the large positive values at 7^oS, 62^oE (warming); Indian Ocean

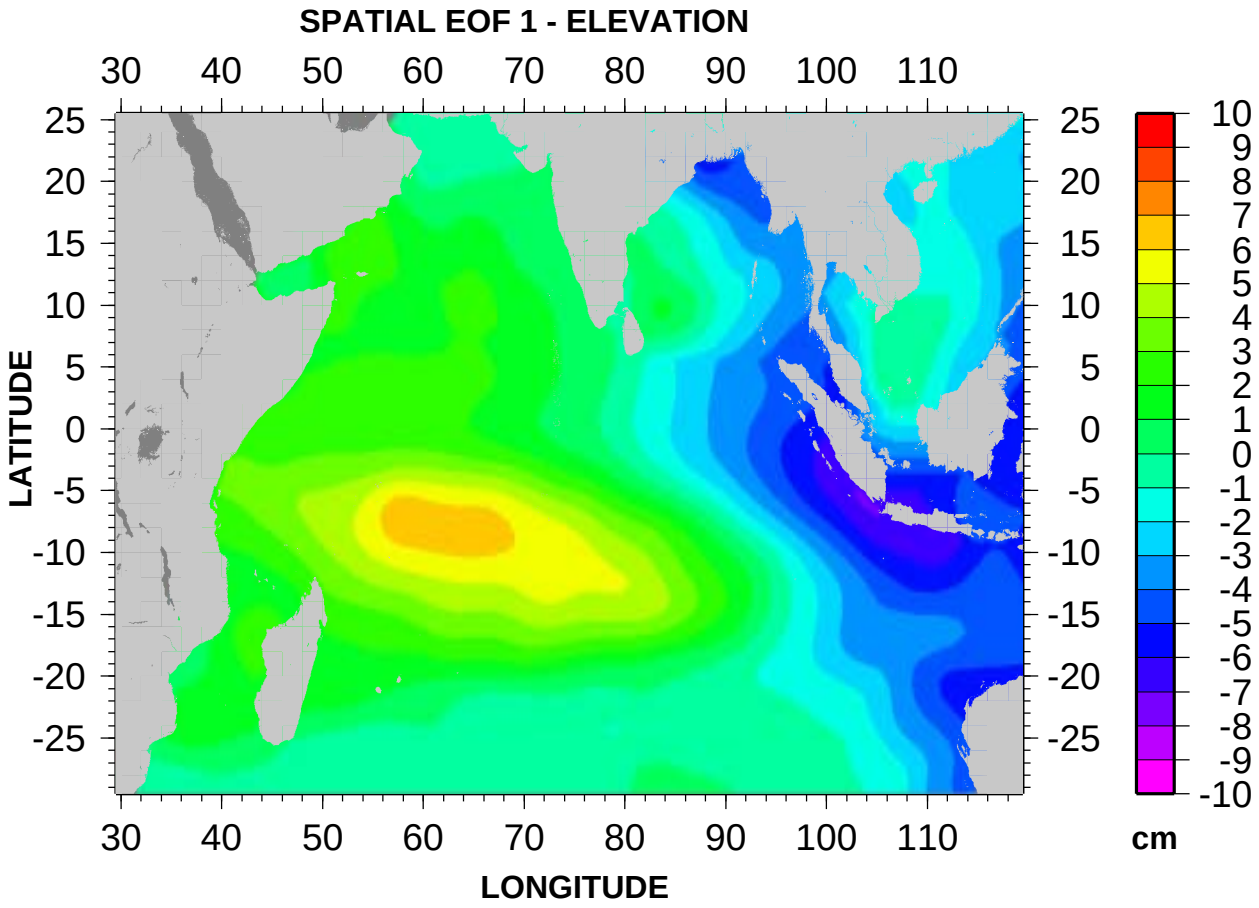

Figure 6.12 EOF analysis: TOPEX/Poseidon sea level height anomaly data - temporal EOF 1 (bottom) & EOF 2 (top) elevation at *interannual* time scales; Indian Ocean

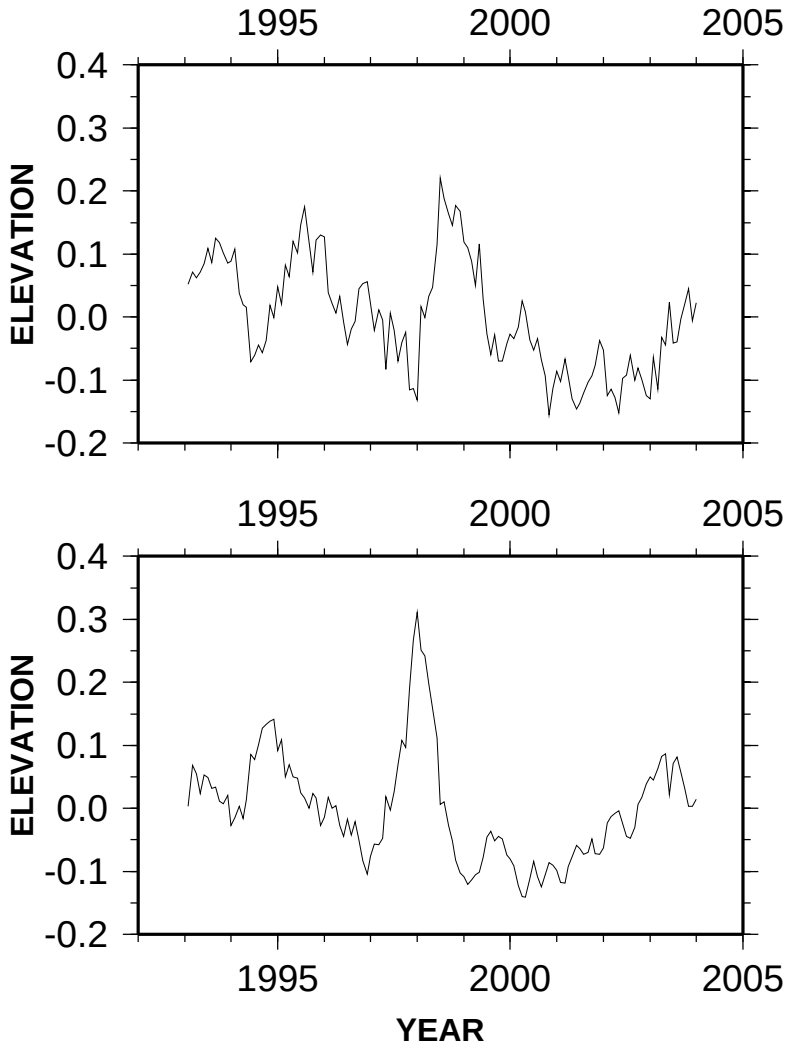

Figure 6.13 EOF analysis: TOPEX/Poseidon sea level height anomaly data - spatial EOF-1 elevation at *interannual* time scales consistent with Chambers et al. [1999] and Picaut et al. [2002]; Pacific Ocean

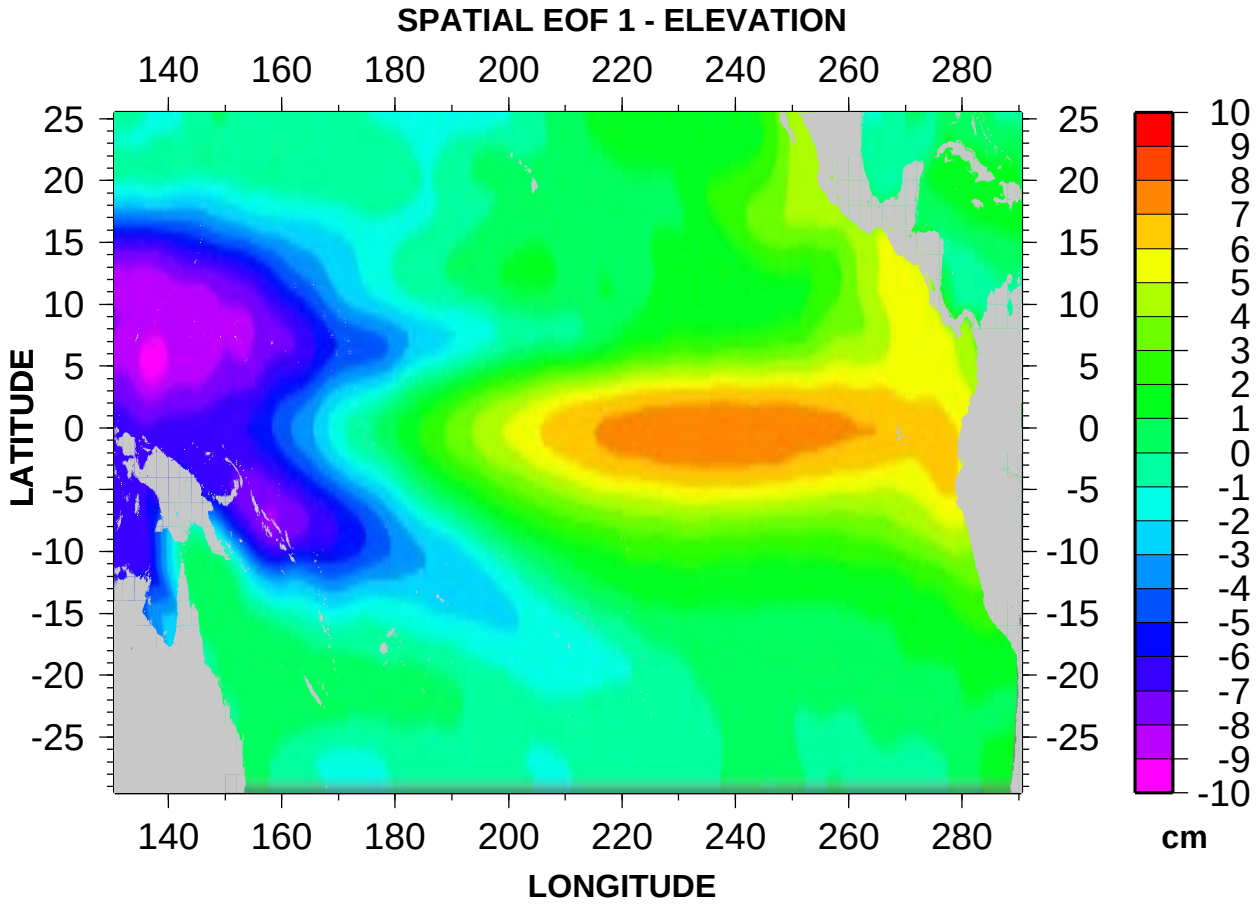

Figure 6.14 EOF analysis: TOPEX/Poseidon sea level height anomaly data - temporal EOF 1 (bottom) & EOF 2 (top) elevation at *interannual* time scales. Note that EOF 1&2 have the signatures of the El Nino and La Nina of the century respectively; Pacific Ocean just like Picaut et al. [2002]

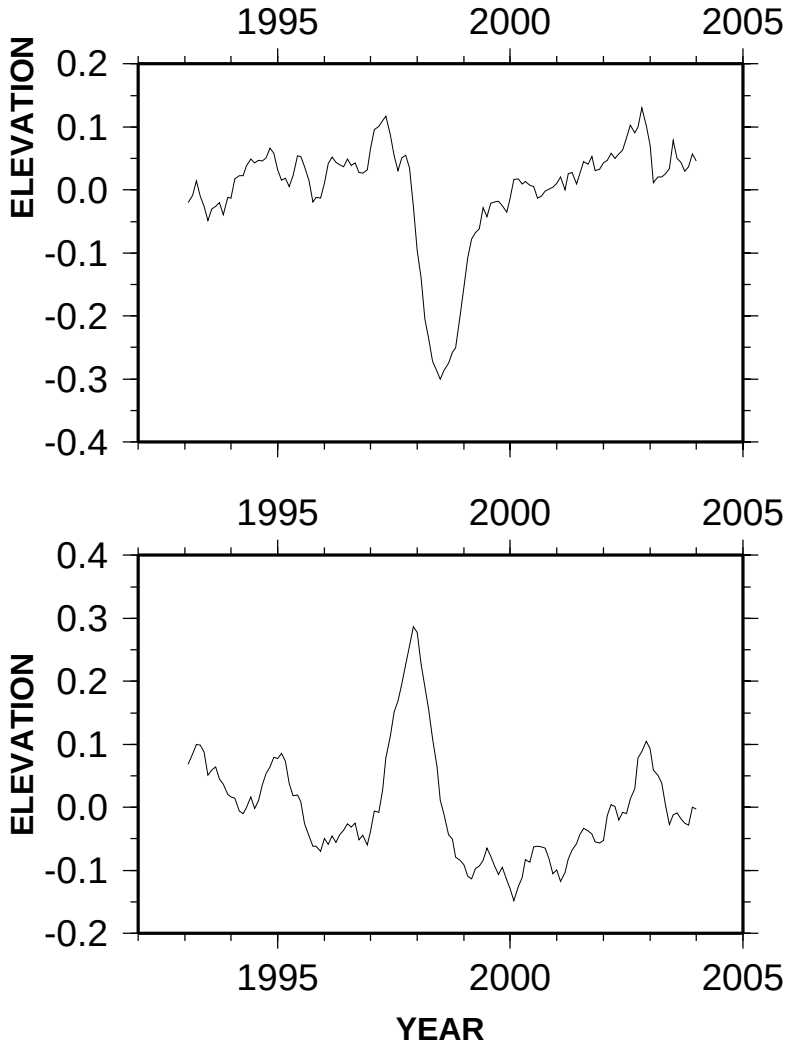

Figure 6.15 EOF analysis: TOPEX/Poseidon sea level height anomaly data - spatial EOF-2 elevation at *interannual* time scales. This spatial EOF corresponds to the La Nina of the century; Pacific Ocean